# $\alpha$ decay of $^{217}$Th populating excited states in $^{213}$Ra

K. Nishio,[1] H. Ikezoe,[1] S. Mitsuoka,[1] and J. Lu[2]
[1]*Advanced Science Research Center, Japan Atomic Energy Research Institute, Tokai-mura, Naka-gun, Ibaraki-ken 319-1195, Japan*
[2]*Instiute of Modern Physics, Chinese Academy of Sciences, 730000 Lanzhou, China*
(Received 7 September 1999; published 17 February 2000)

We have observed the $\alpha$ decay of $^{217}$Th populating the low-lying two excited states in $^{213}$Ra. The branching ratio to the first and the second excited states in $^{213}$Ra, which have expected $J^\pi$ values of $\frac{5}{2}^-$ and $\frac{3}{2}^-$, was determined to be $2.6^{+1.6}_{-1.1}$% and $5.1^{+2.0}_{-1.6}$%, respectively, and the energy of the second excited state in $^{213}$Ra was determined to be 834 keV for the first time. The systematical trend of the branching ratio for $N=125$ isotones with even proton numbers near the $^{208}$Pb core was reasonably explained by the shell model of $\alpha$ decay, where the relative reduced width for specific neutron-orbital and angular momentum has an identical value for the nuclei in the systematics.

PACS number(s): 21.10.Pc, 23.60.+e, 27.80.+w, 25.70.Jj

Experimental investigations of low-lying excited states for the $N=125$ isotones with even proton numbers near the $^{208}$Pb core ($^{207}$Pb, $^{209}$Po, $^{211}$Rn, and $^{213}$Ra) are interesting because of the simplicity of the states at low excitation. The single-particle model predicts that the neutron-hole successively occupies the $3p\frac{1}{2}$, $2f\frac{5}{2}$, and $3p\frac{3}{2}$ orbitals, dominating the configuration of the low-lying states. These states are populated by a $\gamma$ transition following fusion reactions [1] and by particle stripping and/or pickup reactions [2]. Electron capture [3,4] and $\alpha$ decay [4–6] of a precursor also populate these states. The $\alpha$ decay to the $J^\pi=\frac{5}{2}^-$ and $\frac{3}{2}^-$ excited states as well as the ground state in $^{207}$Pb, $^{209}$Po, and $^{211}$Rn have been investigated. On the other hand, for $\alpha$ decay of $^{217}$Th only the decay feeding the ground state in $^{213}$Ra has been reported so far [5,7]. In this paper we have observed the $^{217}$Th $\alpha$ decay populating the low-lying two excited states in $^{213}$Ra, which have an expected spin and parity of $\frac{5}{2}^-$ and $\frac{3}{2}^-$, and the branching ratios to these states were determined. We established the excitation energy of the second excited states in $^{213}$Ra for the first time. Discussions of the systematic trend of the branching ratio for the $N=125$ isotones will be given on the basis of the shell model of $\alpha$ decay

We have performed a $^{28}$Si+$^{198}$Pt fusion reaction to produce $^{217}$Th by the $\alpha5n$ channel. The $^{28}$Si beam of 140–180 MeV was supplied from JAERI-tandem accelerator and used to bombard the rotating $^{198}$Pt targets. The $^{198}$Pt targets of 460 $\mu$g/cm$^2$ thickness were made by sputtering the enriched material of a $^{198}$Pt isotope (98%) on a 0.8 $\mu$m aluminum foil. $^{28}$Si particles used to irradiate the target amounted to $3.6\times10^{15}$–$8.8\times10^{15}$ for each beam energy. The evaporation residues (ER's) emitted to the beam direction were separated in flight from the beam by the recoil mass separator (JAERI-RMS [8]). The separated recoils were implanted into a double-sided position-sensitive strip detector (PSD; 73 $\times55$ mm$^2$). Two larger area timing detectors, one positioned at the front of the PSD and the other 30 cm upstream the PSD, were used to obtain the time-of-flight (TOF) signal of the ER. The two dimensional spectrum of the energy versus TOF discriminated the ER's from the background particles. The TOF response distinguished two types of events: those associated with an ER flying through the separator and those resulting from the $\alpha$ decay of ER's already embedded in the PSD. $\alpha$-decay events longer than 5 $\mu$s life were recorded. Energy calibration of the PSD was made using known $\alpha$ lines from $^{214}$Ra(7.137 MeV), $^{215}$Ra(8.700 MeV), and $^{216}$Th(7.921 MeV) [7]. Gain stability of the detection system was carefully checked by impinging the $^{241}$Am $\alpha$ particles on the PSD. Typical energy resolution of the PSD was 75 keV (full width at half maximum).

Figure 1 shows the excitation curve of $^{217}$Th as a function of c.m. energy $E_{c.m.}$ The absolute cross sections were obtained as shown in Ref. [9]. The solid curve shows the statistical model prediction by HIVAP [10], which agrees with the present data quite well. This calculation indicates that $^{217}$Th is predominantly produced by the $\alpha5n$ channel.

Figure 2(a) shows the typical energy spectrum of $\alpha$-decay events obtained at a beam energy of $E_{c.m.}=147.5$ MeV. $\alpha$ events in Fig. 2(a) are correlated with the implanted ER's within 10 s, and the difference between the position of the $\alpha$ decay and that of the implanted ER is less than $(\Delta X,\Delta Y)$

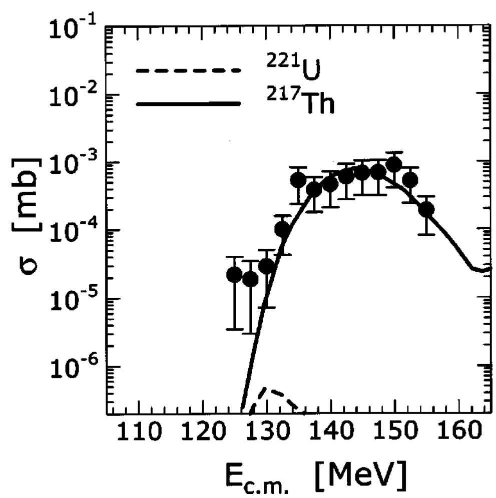


FIG. 1. Cross section versus $E_{c.m.}$ determined from the correlation between the ER event and the $\alpha$ decay of $^{217}$Th. The cross section of the $\alpha5n$ channnel following the $^{28}$Si+$^{198}$Pt fusion reaction is calculated by HIVAP and is shown by the solid curve. The dashed curve is the cross section for $^{221}$U ($5n$ channel).

 

TABLE I. Half-life obtained in this work.

| Nuclei | Half-life in this work | Reference |
|---|---|---|
| $^{215}$Ra | $1.62^{+0.16}_{-0.13}$ ms | $1.56\pm0.10$ ms [6] |
| $^{216}$Th | $22.0^{+1.6}_{-1.4}$ ms | $28\pm2$ ms [5] |
| $^{214}$Ra | $2.10^{+0.09}_{-0.09}$ s | 2.46 s [7] |
| $^{212}$Ra | $11.8^{+1.3}_{-1.0}$ s | 13.0 s [7] |

$=(0.24,0.34)$ mm. We denote the $\alpha$-decay event of ER as $\alpha_1$. Half-lives of $^{216}$Th and $^{215,214}$Ra determined from the ER-$\alpha_1$ correlation are listed in Table I together with the reported data. Table I also includes the half-life of $^{212}$Ra determined from the ER-$\alpha_1$-$\alpha_2$ correlation, where $\alpha_2$ stands for the $\alpha$ decay of the daughter. The measured half-lives agree with those in the references for $^{215,212}$Ra. A trivial difference is found for $^{216}$Th and $^{214}$Ra.

On the events appearing in Fig. 2(a), we impose the condition that the successive $\alpha$ decay have $^{213}$Ra character (daughter of $^{217}$Th). The $^{213}$Ra at ground state has a half-life of 2.74 min [7], which decays by $\alpha$ emission with 80% branch. It has three $\alpha$-decay branches of 6.731 MeV (45%), 6.624 MeV (49%), and 6.522 MeV (6%). Thus the chain ER-$\alpha_1$-$\alpha_2$ of interest has a time interval $\Delta T(\text{ER-}\alpha_1)$ of less than 10 s, $0.274\leqslant\Delta T(\alpha_1\text{-}\alpha_2)\leqslant27.4$ min and $6.422\leqslant E_{\alpha2}\leqslant6.831$ MeV. The position gate of $(\Delta X,\Delta Y)=(0.24,0.34)$ mm was also settled. The result is shown in Fig. 2(b), where the events measured at $E_{\text{c.m.}}=132.5$–$155.0$ MeV are summed. The large peak noted by A is the $\alpha$ decay of $^{217}$Th feeding the ground state in $^{213}$Ra. The average energy is 9.247 MeV, which agrees well with 9.250 MeV in Ref. [7]. In addition to the main peak A, four clusters indicated by B, C, D, and E are observed. Ten events in E were obtained at the energy of $E_{\text{c.m.}}=150.0$, 152.5, and 155.0 MeV. They have half-lives of $T_{1/2}=0.20^{+0.09}_{-0.05}$ s and the average energy is 7.619(32) MeV. We assign this $\alpha$ decay to be $^{215}$Ac ($T_{1/2}=0.17$ s, $E_\alpha=7.604$ MeV), whose daugher $^{211}$Fr decays by $\alpha$ emission with 80% branch ($E_\alpha=6.534$ MeV, $T_{1/2}=3.1$ min [7]). Events in D come from the $^{216}$Th-$^{212}$Ra chain. Since the daughter $^{212}$Ra decays with $E_\alpha=6.899$ MeV and $T_{1/2}=13.0$ s [7], some events should appear in Fig. 2(b). We consider that the clusters indicated by B and C in Fig. 2(b) correspond to the $\alpha$ decay of $^{217}$Th populating the excited states in $^{213}$Ra. The low-lying excited state in $^{213}$Ra populated by the $\alpha$ decay instantaneously decays by $\gamma$ transition and populates the ground state of $^{213}$Ra, followed by $\alpha$ decay with 80% branch. It must be mentioned

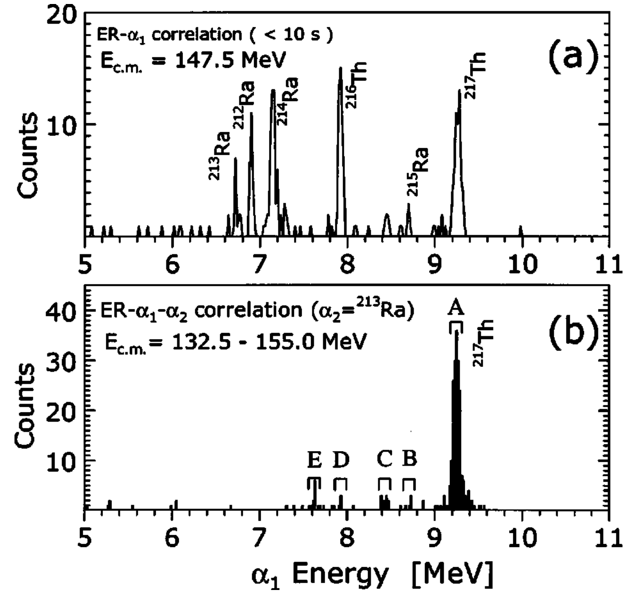


FIG. 2. (a) Energy spectrum of $\alpha$-decay events obtained at $E_{\text{c.m.}}=147.5$ MeV. The events are correlated with the implanted ER's within 10 s and $(\Delta X,\Delta Y)=(0.24,0.34)$ mm. Peaks arising from known $\alpha$ lines are observed. (b) Energy spectrum of $\alpha_1$ obtained in the ER-$\alpha_1-\alpha_2$ chain, where $\alpha_2$ has the character of $\alpha$ decay of $^{213}$Ra. Data obtained at $E_{\text{c.m.}}=132.5$–$155.0$ MeV are summed to yield high statistics.

that the $E_{\alpha1}$ of $^{215}$Ra overlaps with cluster B. However, $\alpha$ decay of $^{215}$Ra does not appear in Fig. 2(b) because the daughter $^{211}$Rn has a long half-life of 14.6 h compared to the present time gate $\Delta T(\alpha_1\text{-}\alpha_2)$. Five events were obtained in B. Among the 11 events in C, one event had the $\Delta T(\text{ER-}\alpha_1)$ of 500 times larger than the others. This event was considered to be a background, thus was not used in the analysis. The average energy and the half-lives of $\alpha_1(^{217}\text{Th})$ decay and $\alpha_2(^{213}\text{Ra})$ decay determined from the ER-$\alpha_1$-$\alpha_2$ chain are summarized in Table II.

The present half-life of $^{217}$Th agrees with 0.252 ms in [5] for every transition. The half-life of $^{213}$Ra for the three transitions also agrees with 2.74 min in Ref. [7]. $\alpha$ decay $Q$ values, $Q_\alpha$, are calculated and listed in Table II, where the screening effect of an electron shelding was corrected by [11]. The first excited state in $^{213}$Ra predicted by the present experiment is 544 keV. This agrees with 546 keV by Raich *et al.* [1] (see Fig. 7 in their paper). They obtained this value by $\gamma$ spectroscopy, where the $J^\pi=\frac{5}{2}^-$ state was fed by $\gamma$ cascade. The second excited state is 834 keV, obtained in the

TABLE II. $\alpha$ energy ($E_\alpha$), half-life ($T_{1/2}$), $Q$ value of $\alpha$ decay ($Q_\alpha$) and the branching ratio for the $\alpha$ decay of $^{217}$Th determined from the ER-$\alpha_1$-$\alpha_2$ events. The half-life for $^{213}$Ra is given in column 6. The last column is the expected neutron orbital in $^{213}$Ra.

| | $E_\alpha$ (MeV) | $T_{1/2}$ (ms) | $Q_\alpha$ (MeV) | Branching ratio (%) | $T_{1/2}$ for $^{213}$Ra (min) | State |
|---|---|---|---|---|---|---|
| A | 9.247(15) | $0.261^{+0.022}_{-0.018}$ | 9.456 | $92.3^{+0.6}_{-0.6}$ | $2.54^{+0.21}_{-0.18}$ | $3p\frac{1}{2}$ |
| B | 8.713(32) | $0.29^{+0.24}_{-0.09}$ | 8.912 | $2.6^{+1.6}_{-1.1}$ | $2.7^{+2.1}_{-0.8}$ | $2f\frac{5}{2}$ |
| C | 8.429(32) | $0.21^{+0.10}_{-0.05}$ | 8.622 | $5.1^{+2.0}_{-1.6}$ | $2.5^{+1.2}_{-0.6}$ | $3p\frac{3}{2}$ |

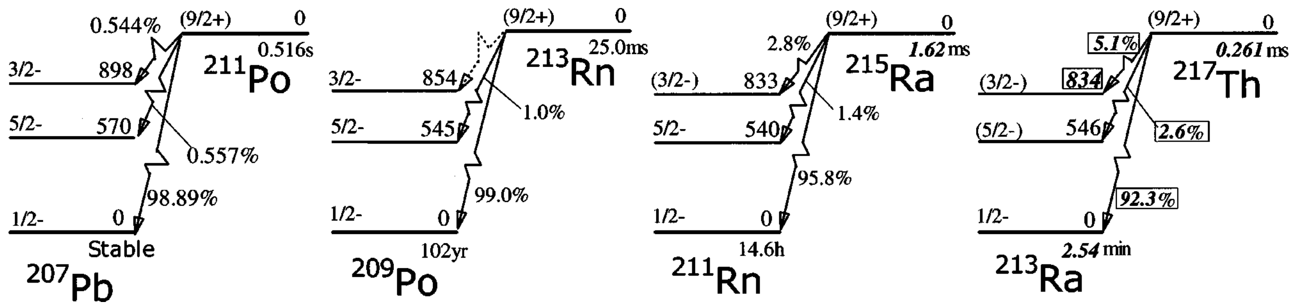


FIG. 3. Low-lying states of $N=125$ isotones with even proton numbers near the $^{208}$Pb core. The branching ratio to these levels populated by $\alpha$ decay is also shown. Numerals indicated by the *italic* symbol represent the present results, in which the quantities in the box represent the first results in this work. Other quantities are taken from Ref. [7]. No data exists for the decay of $^{213}$Rn populating the $J^{\pi}=\frac{3}{2}^{-}$ state in $^{209}$Po.

present experiment for the first time. The branching ratio to these states is listed in Table II. If we assume that the 834 keV level in $^{213}$Ra to have $J^{\pi}=\frac{3}{2}^{-}$, the systematics of low-lying second excited states for $N=125$ isotones with even proton numbers is extended to $Z=88$ as shown in Fig. 3.

In the study of low-lying excited states in $^{213}$Ra by Raich *et al.* [1], they did not find an internal $\gamma$ transition originating from the $J^{\pi}=\frac{3}{2}^{-}$ (834 keV) state. They found the 2.1 ms isomeric state (1770 keV) in $^{213}$Ra, and $J^{\pi}=\frac{17}{2}^{-}$ was suggested for this state. This isomeric state populates the $\frac{9}{2}^{-}$ state of 1608.9 keV directly and/or via the 1769.7 keV ($\frac{13}{2}^{-}$) state by $\gamma$ transition. The 1608.9 keV-level decays to the 546 keV ($\frac{5}{2}^{-}$) state by a $E2\,\gamma$ transition and skips the $\frac{3}{2}^{-}$ states [1]. This hindrance of populating the $\frac{3}{2}^{-}$ state by $\gamma$ cascade is also found in $^{211}$Rn (Fig. 3 in Ref. [12]) and $^{209}$Po (Fig. 3 in Ref. [13]), where the transition arising from the $\frac{3}{2}^{-}$ state (833 keV in $^{211}$Rn and 854 keV in $^{209}$Po) was not seen. The similarity in the hindrance of $\gamma$ transition originating from the state in 830–850 keV through the $N=125$ isotones with an even proton number supports that the level of 834 keV in $^{213}$Ra has the same spin parity, $\frac{3}{2}^{-}$.

For the $\alpha$ decay of $^{213}$Rn, transition to the $\frac{3}{2}^{-}$ (854 keV) state is not reported in Ref. [14]. The corresponding $\alpha$ energy would be 7.249 MeV, determined from the ground-state $\alpha$ energy of 8.088 MeV. Missing the observation of $\alpha$ decay to the 854 keV state is presumably because the branching ratio to this state is low, and furthermore a strong $\alpha$ peak of $^{211}$Po ($E_{\alpha}=7.28$ MeV) appears to cover the corresponding $\alpha$ peak in their experiment (Fig. 13 in their paper).

The following can be found from Fig. 3: (1) the probability of yielding two excited states by $\alpha$ decay increases with adding proton numbers, and (2) for the $\alpha$ decay of $^{215}$Ra and $^{217}$Th, decay to the $\frac{3}{2}^{-}$ states is favored rather than the $\frac{5}{2}^{-}$ state of the daughter nucleus, which forms contrasts to the $^{211}$Po $\alpha$ decay.

We have calculated the branching ratio on the basis of the shell model of $\alpha$ decay assuming the "$\delta$-function" approximation [15]. Since the low-lying states in $^{209}$Po, $^{211}$Rn, and $^{213}$Ra are similar to those in $^{207}$Pb, pure shell-model states can be assumed to calculate the reduced width $\gamma^2$ in the $\alpha$ decay of $^{213}$Rn, $^{215}$Ra, and $^{217}$Th. The reduced width for each state is calculated relative to the ground-state transition. Since only the ratios are interesting, the proton factors cancels out, and the ratio of the reduced widths $\gamma^2/\gamma^2_{\mathrm{g.s.}}$ depends only on one of the final states of the neutron orbital. Torgensen and Macfarlane [6] calculated $\gamma^2/\gamma^2_{\mathrm{g.s.}}$ in their study of $^{215}$Ra $\alpha$ decay, where wave functions by Blomqvist and Wahlborn [16] were used. Their calculated $\gamma^2/\gamma^2_{\mathrm{g.s.}}$ values were adopted in this study. Relative penetrability factors $P/P_{\mathrm{g.s.}}$ was calculated by using Rasmussen potential [17] and were multiplied by $\gamma^2/\gamma^2_{g.s.}$ to yield the intensities for each $\alpha$-$l$ wave. The contribution from each $l$ wave is then summed to determine the branching ratio. Figure 4 shows the calculated results of the branching ratios populating $J^{\pi}=\frac{5}{2}^{-}$ (solid) and $\frac{3}{2}^{-}$ (dashed) states as well as the experimental values (triangle: $\frac{5}{2}^{-}$, circle: $\frac{3}{2}^{-}$) as a function of the proton number of the daughter nucleus. The increasing trend of the branching ratio with a proton number is demonstrated by the calculation. Furthermore, the strength populating the $\frac{3}{2}^{-}$ state is larger than that for the $\frac{5}{2}^{-}$ state in $Z\geqslant 86$, which is consistent with the experimental results. As the relative reduced widths $\gamma^2/\gamma^2_{\mathrm{g.s.}}$ are fixed for specific neutron-orbital and angular momentum for these isotones, the systematic change with respect to the proton numbers is governed by $P/P_{\mathrm{g.s.}}$ in the calculation.

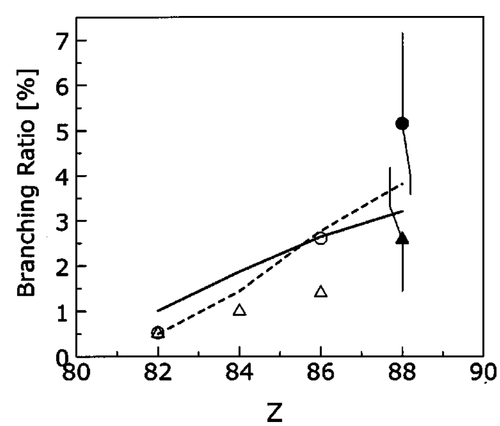


FIG. 4. Branching ratio to $J^{\pi}=\frac{5}{2}^{-}$ and $\frac{3}{2}^{-}$ levels as a function of the proton number of the daughter nucleus. Calculated results based on the shell model of $\alpha$ decay are shown by solid ($\frac{5}{2}^{-}$) and dashed ($\frac{3}{2}^{-}$) curves. Experimental results are shown by triangles ($\frac{5}{2}^{-}$) and circles ($\frac{3}{2}^{-}$), where the present results are shown by a solid symbol with error bar.

In summary, by using the $^{28}Si+^{198}Pt$ fusion reaction we have observed the $\alpha$ decay of $^{217}Th$ populating the low-lying two excited states in $^{213}Ra$ and the branching ratio to the first and the second excited states was determined to be $2.6^{+1.6}_{-1.1}$% and $5.1^{+2.0}_{-1.6}$%, respectively. We established 834 keV for the second excited state in $^{213}Ra$, which has an expected spin-parity of $\frac{3}{2}^-$. The systematical trend of the branching ratio for $N=125$ isotones with even proton numbers was reasonably explained by the shell model of $\alpha$ decay, in which the relative reduced width for specific neutron-orbital and angular momentum was assumed to have identical value for the nuclei in the systematics, indicating that these nuclei at low-excitation has the same shell-structure.

Special thanks are due to Dr. Ishii of JAERI for the fruitful discussion. The authors are indebted to the staff of JAERI tandem facility for providing the $^{28}Si$ beams and for technical assistance.

[1] D. G. Raich, H. R. Bowman, R. E. Eppley, J. O. Rasmussen, and I. Pezanka, Z. Phys. A **279**, 301 (1976).
[2] T. S. Bhatia, T. R. Canada, P. D. Barnes, R. A. Eisenstein, and C. Ellegaard, Nucl. Phys. **A314**, 101 (1979).
[3] L. J. Jardine, S. G. Prussin, and J. M. Hollander, Nucl. Phys. **A233**, 25 (1974).
[4] L. J. Jardine, Phys. Rev. C **11**, 1385 (1975).
[5] K. Valli and E. K. Hyde, Phys. Rev. **176**, 1377 (1968).
[6] D. F. Torgensen and R. D. Macfarlane, Phys. Rev. C **2**, 2309 (1970).
[7] R. B. Firestone, *Table of Isotopes*, edited by V. S. Shirley (Wiley, New York, 1996).
[8] H. Ikezoe, Y. Nagame, T. Ikuta, S. Hamada, I. Nishinaka, and T. Ohtsuki, Nucl. Instrum. Methods Phys. Res. A **376**, 420 (1996).
[9] T. Kuzumaki, H. Ikezoe, S. Mitsuoka, T. Ikuta, S. Hamada, Y. Nagame, I. Nishinaka, T. Ohtsuki, and O. Hashimoto, Nucl. Instrum. Methods Phys. Res. A **437**, 107 (1999).
[10] W. Reisdorf and M. Scädel, Z. Phys. A **343**, 47 (1992).
[11] J. O. Rasmussen, *Alpha-, Beta-, and Gamma-Ray Spectroscopy*, Vol. 1 (North-Holland, Amsterdam, 1966), Chap. XI.
[12] A. R. Poletti, G. D. Dracoulis, C. Fahlander, and I. Morrison, Nucl. Phys. **A359**, 180 (1981).
[13] T. Yamazaki and E. Matthias, Phys. Rev. **175**, 1476 (1968).
[14] K. Valli, E. K. Hyde, and J. Borggreen, Phys. Rev. C **1**, 2115 (1970).
[15] J. O. Rasmussen, Nucl. Phys. **44**, 93 (1963).
[16] J. Blomqvist and S. Wahlborn, Ark. Fys. **16**, 545 (1960).
[17] J. O. Rasmussen, Phys. Rev. **115**, 1675 (1959).